Contact Guidance Diversity in Rotationally Aligned Collagen Matrices

Jacob A.M. Nuhn[1], Anai M. Perez[3] and Ian C. Schneider[1,2*‡]

[1]Department of Chemical and Biological Engineering, Iowa State University

[2]Department of Genetics, Development and Cell Biology, Iowa State University

[3]Department of Chemistry and Physics, Grand View University

*Present address: Iowa State University, Department of Chemical and Biological Engineering, 2114 Sweeney Hall, Ames, IA, 50011-2230

‡Author for correspondence (phone: (515) 294-0450, fax: (515) 294-2689, e-mail: ians@iastate.edu

Abstract:

Cancer cell metastasis is responsible for approximately 90% of deaths related to cancer. The migration of cancer cells away from the primary tumor and into healthy tissue is driven in part by contact guidance, or directed migration in response to aligned extracellular matrix. While contact guidance has been a focus of many studies, much of this research has explored environments that present 2D contact guidance structures. Contact guidance environments in 3D more closely resemble *in vivo* conditions and model cell-ECM interactions better than 2D environments. While most cells engage in directed migration on potent 2D contact guidance cues, there is diversity in response to contact guidance cues based on whether the cell migrates with a mesenchymal or amoeboid migration mode. In this paper, rotational alignment of collagen gels was used to study the differences in contact guidance between MDA-MB-231 (mesenchymal) and MTLn3 (amoeboid) cells. MDA-MB-231 cells migrate with high directional fidelity in aligned collagen gels, while MTLn3 cells show no directional migration. The collagen stiffness was increased through glycation, resulting in decreased MDA-MB-231 directionality in aligned collagen gels. Interestingly, partial inhibition of cell contractility dramatically decreased directionality in MDA-MB-231 cells. The directionality of MDA-MB-231 cells was most sensitive to ROCK inhibition, but unlike in 2D contact guidance environments, cell directionality and speed are more tightly coupled. Modulation of the contractile apparatus appears to more potently affect contact guidance than modulation of extracellular mechanical properties of the contact guidance cue.

Statement of Significance:

Collagen fiber alignment in the tumor microenvironment directs migration, a process called contact guidance, enhancing the efficiency of cancer invasion and metastasis. 3D systems that assess contact guidance by locally orienting collagen fiber alignment are lacking. Furthermore, cell type differences and the role of extracellular matrix stiffness in tuning contact guidance fidelity are not well characterized. In this paper rotational alignment of collagen fibers is used as a 3D contact guidance cue to illuminate cell type differences and the role of extracellular matrix stiffness in guiding cell migration along aligned fibers of collagen. This local alignment offers a simple approach by which to couple collagen alignment with gradients in other directional cues in devices such as microfluidic chambers.

Graphical Abstract:

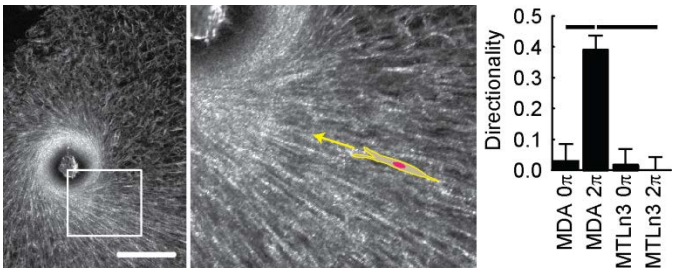

Key Words:

Directed motility; three-dimensional; acupuncture; glycation; stiffness; confocal reflectance microscopy; breast cancer; orientation; blebbistatin; Y-27632

1. Introduction:

Cancer cell metastasis is responsible for 90% of fatalities related to cancer [1]. Mimicking metastasis in engineered environments to separate or expand patient-derived cells, identifying metastatic diagnostic signatures and designing therapeutics that target metastasis is crucial to limiting cancer's effects on public health. The complex and diverse migratory behavior that leads to metastasis has begun to be described by a reduced set of cell phenotypes called modes of migration. There are two main migration modes which have been identified as important in the metastasis of cancer cells: mesenchymal and amoeboid [2]. The mesenchymal mode of migration is typified by a spindle-like morphology, where cells protrude and retract multiple simultaneously existing extensions. Mesenchymal mode migrators seem to be highly adhesive and contractile, remodeling matrix by exerting large traction forces. These cells also rely on matrix degradation that is coupled to matrix remodeling through traction forces. The amoeboid mode of migration is typified by a rounded morphology, where cells generally extend one pseudopod-like structure. Amoeboid mode migrators are less adhesive and the contractility is not devoted to traction force generation, so much as it is to cytoskeletal-mediated squeezing, producing movement of the cell body toward the extended pseudopod [3]. Contact guidance, or directed migration along aligned fibers, has been shown to play a large role in some metastatic cancers. For instance, in breast cancers [4], stromal and cancer cells cooperate to orient collagen fibers perpendicular to the tumor margin and cancer cells use this directional cue to migrate from the primary tumor. *In vitro* models of tumors also show radial fiber alignment [5]. It is becoming more appreciated that cells with different migration modes may respond to contact guidance cues with much different fidelities. Cell type differences in contact guidance have been observed for quite some time. More recently, we and others have shown that motility mode can predict the fidelity of contact guidance, even in situations where migration speed is similar [6-8]. This suggests that metastasis as driven by structural changes in the collagen fiber orientation may only be potent for certain cell phenotypes.

In addition to structural organization of collagen fibers, the tumor microenvironment tends to be stiffer in highly invasive cancers as compared to normal tissue [9, 10]. It has long been known that the stiffness of the extracellular matrix (ECM) can have a profound influence on cell morphology and migration [11-14]. Model 2D flexible substrates including polyacrylamide and polydimethylsiloxane have been used frequently to uncover the effects of stiffness on cell function. Controlling stiffness in 3D environments like collagen gels is a bit more difficult. Increasing collagen concentration results in stiffer gels, but the ligand density for receptor binding is also different, convoluting chemical and physical cues. Collagen gels can also be crosslinked by chemicals or enzymes; however this crosslinking is frequently done in the presence of cells and can present some practical difficulties. Recently, glycation has been used to increase the stiffness of collagen gels [15]. Collagen can be non-enzymatically functionalized with

ribose, resulting in a stiffer gel, while keeping the collagen concentration and consequently, ligand density the same. This approach has been used frequently to assess the role of the mechanical properties of the collagen gel in controlling cell function including cell migration. While the role of stiffness in controlling cell migration is relatively well-known, it is unknown how stiffness affects contact guidance. Do networks with the same collagen structure, but different stiffness result in different contact guidance?

Predicting how a cell's migratory mode as well as how the ECM stiffness affects migration behavior requires understanding how a cell's cytoskeletal structures function. Cells adhere to collagen fibers using integrins and discoidin domain receptors on the surface of the cell. Receptor binding leads to focal adhesion assembly that is linked to a contractile F-actin cytoskeletal network, allowing for the cell to transmit force to the surroundings [16, 17]. Mesenchymal cells have shown a propensity to form strong bonds with their surroundings, allowing them to remodel the matrix while they migrate [18]. Amoeboid cells bind the ECM with less force and use a number of physical mechanisms such as contraction-based blebbing or squeezing [19]. These differences between the two modes lead mesenchymal cells to form much stronger attachments to the ECM and allow them to respond more robustly to directional cues from aligned fibers. Contractility is generated through myosin II-mediated contraction of the F-actin cytoskeleton. Several signaling proteins including kinases such as Rho kinase (ROCK) can dynamically regulate contractility through phosphorylation of myosin II regulatory light chain and we have shown this to be important in contact guidance on 2D substrates [6]. Others have shown contractility to be important in 3D contact guidance environments [20].

In vivo, the ECM environment is compositionally, structurally and mechanically complex. This complexity has forced many simplifications in *in vitro* systems. For instance, most of the research conducted with regards to contact guidance has focused on 2D models. 2D models provide finer and more reproducible control than 3D models over structural properties of the contact guidance cue including fiber size and orientation. The most common 2D systems for studying contact guidance include gratings coated with ECM, microcontact printed lines of ECM and epitaxial grown collagen fibers [7, 21-23]. 3D systems are more difficult to control and image through, but several have been devised including cell-based, flow-based and magnetic orientation of contact guidance cues [8, 20, 24-27]. Cell-based systems provide little tunable control over the orientation of the ECM and require decellularization. Flow-based systems commonly require microfluidic devices and small length scales over which ECM orientation occurs. Magnetic fields alone or in combination with iron oxide particles can generate aligned collagen networks. However, these require either large magnetic fields or particles that could perturb cell behavior. Another intriguing approach is to use rotational alignment imparted by an acupuncture needle [28, 29]. When an acupuncture needle is inserted into a collagen gel, collagen fibers adhere to the surface. During rotation collagen fibers are wrapped around the needle generating alignment of the fiber network. This approach

has been used to both assess the role of acupuncture in eliciting cell biological responses [30] and has been used to show directional orientation of fibroblasts in oriented collagen gels [28, 29]. In this paper, we use rotational alignment of collagen fibers to assess contact guidance. We quantify the alignment of collagen fiber networks and use them to assess how mesenchymal and amoeboid cells differ in their ability to engage in contact guidance. Furthermore, we examine the effects of tuning extracellular stiffness and intracellular contractility on contact guidance fidelity and attempt to parse different contributions of these perturbations to both random and directional aspects of cell migration.

2. Material and Methods:

2.1 Culturing Cells

MDA-MB-231 cells (human mammary basal/claudin low carcinoma cells, ATCC, Manassas, VA, USA) were cultured using Dulbecco's Modified Eagles Medium (DMEM) (Sigma Aldrich, St. Louis, MO, USA) with 10% fetal bovine serum (FBS) (Gibco, Grand Island, NY, USA), 2% glutamax (Gibco) and 1% penicillin/streptomycin (Gibco). Imaging media used for experiments consisted of DMEM lacking phenol red, supplemented with 10% FBS, 2% Glutamax, 1% penicillin/streptomycin, 1% sodium pyruvate (Gibco), and 12 mM HEPES (Sigma Aldrich).

MTLn3 cells (rat mammary basal adenocarcinoma cells, Jeffrey Segall, Albert Einstein College of Medicine and authenticated using IDEXX BioResearch, Westbrook, Maine, USA) were cultured using MEMα media (Sigma Aldrich) supplemented with 5% FBS and 1% penicillin/streptomycin. Imaging media used for experiments consisted of MEM alpha lacking phenol red, supplemented with 5% FBS, 1% penicillin/streptomycin, and 12 mM HEPES. Mycoplasma was tested using a MycoFluor myocoplasma detection kit (Invitrogen, Carlsbad, CA, USA) and no mycoplasma were detected.

2.2 Sample Preparation for Confocal Microscopy

Confocal experiments were prepared by mixing imaging media and non-pepsin-treated rat collagen type I solution (Corning, Corning, NY, USA) to a concentration of 2 mg ml^{-1}. A volume of collagen solution (125 μl) was pipetted into a MatTek dish. MatTek dishes are conventional 35 mm tissue culture dishes with a hole in the bottom that is covered with a glass coverslip. This coverslip is glued to the bottom, creating a shallow well (MatTek Corporation, Ashland, MA, USA). Collagen is spread evenly on the bottom of the well, and allowed to polymerize for 45 mins. A 0.25 x 25 mm stainless steel acupuncture needle with a tapered tip (Hwato, Weymouth, MA, USA) was inserted through a 5 mm thick pad of polydimethylsiloxane (PDMS) (Dow Corning Corporation, Midland, MI, USA) to the depth of the well and placed on top of the collagen gel, sealed with food grade lubricant (The McGlaughlin Oil Company, Columbus, OH, USA). The needle was then rotated the required degrees slowly to limit the amount of gel tearing and cut with wire cutters.

2.2 Confocal Microscopy and Analysis

Confocal reflectance microscopy was used to determine the degree of collagen fiber alignment. At least four samples of each condition were imaged on a Leica SP5 X MP confocal/multiphoton microscope system with a 40X (*NA* = 1.25) oil immersion objective. Images with significant tearing, due to the needle tip dragging when it was cut were removed from analysis. In addition, images were discarded if the ripped area was larger than 25% of the total image area due to needle rotation. The images were then

averaged using a Gaussian blur filter with a standard deviation of 2 and analyzed with the ImageJ plugin OrientationJ [31] with a cubic spline gradient and a Gaussian window of 4 pixels. The coherency and orientation images were then saved and used later in the analysis. A Matlab (Mathworks, Natick, MA, USA) script was written which identifies average collagen fiber orientation and builds a circumferential vector field. The coherency and orientation images were then used to compare the fiber orientation to a circumferential vector field using coherency cutoff of 0.2. The angle between the local collagen fiber orientation vector and a circumferential vector field is θ_f. The directionality of the fiber field was defined in the following way.

$$DI_f = \cos\theta_f \quad (1)$$

When the fiber orientation is circumferential, the DI_f is 1 and when the fiber orientation is radial, the DI_f is 0.

2.3 Cell Migration Sample Preparation

Cell migration experiments were conducted by mixing trypsinized cells at a concentration of at 600,000 cells ml^{-1} in a 2 mg ml^{-1} non-pepsin-treated rat collagen type I solution (Corning, Corning, NY, USA). The protocol is similar to the confocal experiments, however after polymerization the well is filled with 125 ml of imaging media specific to the cell type. The needle is either not rotated or rotated one full rotation (2π) and then cut by wire cutters. The samples are then placed in a 37 °C incubator. After 24 hr the samples are moved to a heating stage to keep the samples at 37 °C and imaged every 2 min for 8 hr. At least 3 samples over at least 2 different days compiled a complete data set.

2.4 Collagen Glycation Procedure

Collagen fiber stiffness was controlled by glycating collagen. Non-pepsin-treated rat collagen type I solution was diluted with ribose dissolved in nanopure water at a concentration of 200 mM, resulting in a collagen concentration of 7 mg ml^{-1} and lowering the acetic acid concentration which the collagen is diluted in from 0.02 N to 0.015 N. This solution was allowed to react for 5 days at 4 °C. The glycation occurs through the reduction of sugar, crosslinking collagen fibers which increases the stiffness of the gel by enhancing collagen-collagen interactions without changing other important properties such as pore size or collagen density [15, 32]. This collagen was then used in place of non-glycated collagen and the procedure was completed as previously described with alignment following collagen polymerization.

2.5 Contractility Inhibition

Contractility was inhibited by subjecting cells to Y-27632 (Calbiochem, Billerica, MA, USA) and blebbistatin (Sigma). Cells were suspended in a 1 μM solution of Y-27632 or 3 μM solution of blebbistatin prior to the 24 hr incubation. We have shown these concentrations to partially block contact guidance on 2D surfaces [6].

2.6 Cell Migration Analysis

Analysis of cell migration was conducted using the MTrackJ plugin in ImageJ (National Institutes of Health, Bethesda, MD, USA) which allows the tracking of cells on an image-by-image basis. The result of this is the *x*-*y* coordinates of the cell at each time point. Two migration characteristics were calculated. The first was a random migration parameter, cell speed. The second was a directed migration parameter and quantifies the projection of the migration direction towards the collagen alignment, cell directionality. These points are then analyzed using a custom Matlab script which calculates the quotient of the distance the cell moves between each image and the time interval. When this is averaged over the entire timelapse, an average cell speed is calculated. A Matlab script was written which determines the cell directionality using a similar approach to measuring collagen fiber directionality. A cell's movement direction over a time interval of 24 min was compared to the direction of a radial vector field originating from the needles center to calculate directionality using the following equation.

$$DI_c = \cos 2\theta_c \tag{2}$$

Aspect ratio was calculated by dividing the length of a cell by the width of that same cell.

2.7 Statistical Methods

Confidence intervals (95%) were calculated using Matlab. A two tailed *t*-test, $p \leq 0.05$, was conducted for experiments which only compared two conditions while an Anova test, $p \leq 0.05$ was conducted for experiments which had more than two conditions. These are used to identify statistical differences which were depicted with connecting bars over the particular conditions. Details of the number of samples and experiments are included in the figure legends

3. Results

3.1 Rotation of Acupuncture Needles Align Collagen Fibers

We have used a method which allows for direct manipulation of the alignment of collagen gels through the rotation of an inserted acupuncture needle resulting in a fibrous radial pattern extending from the needle surface to investigate the role of contact guidance on metastatic cancer cells. To achieve radial alignment of the collagen fibers an acupuncture needle is inserted into a gel and rotated clockwise (Figure 1A). Collagen adheres to the needle surface, creating mechanical attachment for force transfer between the needle and the gel. After needle rotation, the fibers should no longer exhibit a random orientation, but instead show directional orientation (Figure 1B&C). Fibers immediately near the needle should show circumferential alignment as the fibers are wound around the needle. Fibers further from the needle should show a radial alignment with slight directional variations caused by the entangled, but incompletely mechanically coupled gel.

Confocal reflectance microscopy was used to image the collagen fibers and gain an understanding of how the insertion of the needle and the time at which the needle is rotated affects the formation of the oriented collagen fiber field. We collected a series of images of gels without any needle insertion, with a needle, but without any rotation, with rotation before the collagen has fully polymerized into a gel, and with rotation after 45 mins of polymerization (Fig 2A-D). The images are taken within approximately 100 μm of the glass-gel interface. The needle is often shown as a bright white spot, although at times a dark hole is present, due to small movement by the needle in the *z*-direction away from the surface. Small changes in fiber directionality are difficult to discern visually, so fiber directionality (DI_f) was calculated using the cosine of the angle between the circumferential direction and fiber direction as a function of distance from the center of the needle and averaged over several experiments. When fiber directionality has a value of 1, fibers are oriented circumferentially. When fiber directionality has a value of 0, fibers are oriented radially. The fiber directionality as a function of distance from the needle center for two conditions (no needle and a rotated needle before collagen is fully polymerized) is shown in Figure 2E. Fiber directionality changes as a function of the distance from the needle center, where regions close to the needle have higher fiber directionality (circumferential orientation) than regions further away from the surface (radial orientation). The surface of the needle falls within the dotted line in Figure 2E, which represents the average needle radius +/- the standard deviation. Fiber directionality to the left of this dotted box was ignored, because this represents a region within the needle and not actual collagen fibers. A slope can be used to characterize the change in fiber directionality as a function of distance from the needle center. When the needle is not inserted the slope is approximately 0 (Figure 2F). Needle insertion does not change the slope. However, needle rotation, even before full collagen polymerization results in a non-zero, negative slope, indicating some alignment. Furthermore, rotation after 45 min of polymerization

results in a large negative slope (Figure 2F). In addition to slope, the fiber directionality at 100 μm from the needle center (DI_{100}) was calculated. Conditions that showed rotation resulted in the lowest DI_{100} values (Figure 2G). Next, we wanted to determined how different degrees of rotation affected collagen alignment (Figure 3A-F). When the needle was rotated one full rotation (2π), it resulted in both higher circumferential alignment closer to the needle (higher DI_f) and higher radial alignment away from the needle as compared to the no rotation control (higher DI_f, Figure 3G). All rotation magnitudes that we probed resulted in a large negative slope (Figure 3G). The DI_{100} values were much more variable and closer to the zero rotation condition, but also decreased (Figure 3I). However, while large degrees of rotation showed dramatic radial alignment (Figure 3F), we observed more tearing of the gel either proximal or distal to the needle under this condition, so an intermediate level of rotation (2π) was used for the cell studies.

3.2 MDA-MB-231 Cells Respond to 3D Contact Guidance Cues, but MTLn3 Cells Do Not

It was important to identify the time over which cells attach and engage in contact guidance in the radially aligned gels. MDA-MB-231 cells were seeded in the gels and imaged prior to, immediately after, and at ~24 hr after rotation (Figure 4A-C). Elongation, as measured by cell aspect ratio, only occurred after ~24 hr after rotation (Figure 4G). This confirms that the act of rotating the needle isn't responsible for the elongation of the cells within the gel. To further confirm the claim that the needle rotation had no effect on cell morphology, a needle was inserted and left unspun for 24 hours allowing the cells to interact with the ECM. The cells were then imaged prior to, immediately after, and at ~24 hr after after rotation (Figure 4D-F). Little difference is seen in the aspect ratio after cells have attached to the ECM, indicating that the mechanical movement of collagen fibers does not act to elongate cells, even when they are well-attached to the ECM (Figure 4G).

Armed with the information that the collagen gel can be aligned by rotating an acupuncture needle and that cell elongation occurred ~24 hr after rotation, we next wanted to see if the collagen alignment induced contact guidance. We measured contact guidance by analyzing the directionality of cells using live cell imaging. Figure 5A&B show the cell tracks from three different experiments after 0π and 2π needle rotations. Cells migrate under both conditions, but the tracks are in the direction of the needle in the gels where needles have been rotated 2π and where radial collagen alignment with respect to the needle occurs (Figure 5B, black arrowhead). Tracks of cells in gels can be persistent, but not directed to the needle with no radial collagen alignment (Figure 5A, black arrowhead). Furthermore, while cells are elongated when the collagen gel is not radially aligned (Figure 5C-F), radial collagen alignment produces persistent migration toward or away from the needle (Figure 5G-J). There appears to be only a slight bias for migration towards the needle. Cell speed was quantified and calculated under both

conditions (Figure 5K). Cell migration speed was over 2-fold faster under radial alignment conditions (Figure 5K). In addition to changes in cell speed, cell directionality was dramatically increased when the needle was rotated 2π and the collagen gel was radially aligned (Figure 5L). The directionality when the needle was not rotated was not statistically different from 0, a value of directionality for random migration. We have shown contact guidance differences between MDA-MB-231 and MTLn3 cells on 2D collagen fibril forming substrates, attributed this in part to their different migratory modes (mesenchymal vs. amoeboid) [7]. Given this difference seen in 2D, we were interested in whether this relationship was seen in 3D, so we probed contact guidance in MTLn3 cells.

Amoeboid MTLn3 cells were subjected to the same conditions as the mesenchymal MDA-MB-231 cells (Figures 6A-D). The differences in morphology are easy to see. MDA-MB-231 cells are spindle-shaped with multiple extensions in the front and usually one tail (Figure 6A&C). MTLn3 cells on the other hand are relatively round with few long extensions, even in the presence of radially aligned collagen fibers (Figure 6B&D). Two possibilities could explain this. First, MTLn3 cells could be non-migratory within the collagen gel. However, MTLn3 cells did migrate and at speeds around those seen for MDA-MB-231 cells (Figure 6E). Second, MTLn3 cells could be highly directional even though they are not well attached to the collagen matrix. However, the directionality of MTLn3 cells was not sensitive to whether the collagen gel was radially aligned and the directionality was similar to that seen for MDA-MB-231 cells in unaligned collagen gels (Figure 6F). The value for directionality of the MTLn3 cells is not statistically different from 0, which is the value of directionality for random migration. Aspect ratios of the MDA-MB-231 and MTLn3 cells also point to the differences in migration mode (Figure 6G). MTLn3 cells have aspect ratios around 1, which correspond to a circular geometry, whereas MDA-MB-231 cells tend to be about 4-6 times longer than they are wide.

3.3 Role of Extracellular Stiffness and Intracellular Contractility in Driving 3D Contact Guidance

We next wanted to investigate how ECM stiffness affects contact guidance of MDA-MB-231 and MTLn3 cells. To achieve this end we used non-enzymatic glycation to stiffen collagen gels [32, 33]. This allowed us to use the same collagen concentration while increasing the collagen stiffness independently. Furthermore, collagen glycation did not seem to alter the structural alignment caused by needle rotation (Figure 7E&F). Given the results mentioned above, we were curious as to whether increases in stiffness affected migration in both cell types. Changes in stiffness through glycation did not seem to alter the morphology greatly (Figure 7A-D). Cell migration speed in MDA-MB-231 cells increased in unaligned and glycated collagen networks as compared to unaligned networks alone, but decreased in aligned and glycated collagen networks as compared to aligned networks alone (Figure 7G). On the other hand, glycation resulted in increasing MTLn3 cell speed in both unaligned and aligned collagen networks

(Figure 7J). Interestingly, this effect on speed looks to be approximately additive, where the increase in speed in glycated or aligned collagen networks can be summed to predict the speed for glycated and aligned collagen networks. Both directionality and elongation were diminished in MDA-MB-231 cells with collagen glycation and increased stiffness, indicating that the directional aspect of contact guidance is sensitive to network stiffness (Figure 7H-I&K-L).

After examining how cells respond to a stiffer collagen matrix, we wanted to determine if internal changes in myosin II-mediated contractility mirrored changes in contact guidance seen with external changes in matrix stiffness. Indeed, we and others have shown that myosin inhibition alters directional migration on 2D contact guidance cues [6]. To achieve this, MDA-MB-231 cells were exposed to two contractility inhibitors, blebbistatin (a myosin II inhibitor) and Y-27632 (a Rho kinase inhibitor) and seeded in unaligned and aligned collagen gels (Figure 8A-D). We chose inhibitor concentrations that are known to only partially block contractility [6]. Both drugs eliminated the speed differences seen between unaligned and aligned collagen networks, although Rho-kinase inhibition resulted in lower speeds (Figure 8E). However, the most striking result of limiting the contractility is the marked decrease in directionality in response to Y-27632 (Figure 8F). Y-27632 almost completely transformed the response of MDA-MB-231 cells to an aligned collagen network to that of an unaligned collagen network (Figure 8F). Blebbistatin on the other hand was much less effective in deceasing both speed and directionality. The response of aspect ratio to contractility inhibitors was similar to directionality, indicating that elongation in aligned collagen networks is a likely proxy for directionality (Figure 8G). This can be more easily shown when aspect ratio and directionality for all conditions probed above are plotted against each other for both unaligned (grey) and aligned (black) collagen gels (Figure 9A). A clear linear and increasing relationship is seen in aligned collagen networks, whereas no linear relationship is seen in unaligned collagen networks across all conditions.

4. Discussion:

In this paper we present results assessing contact guidance in a 3D ECM environment. 2D systems, while shedding some light on how cells engage in contact guidance, neglect many important characteristics observed *in vivo*. Rotational alignment of the ECM using acupuncture needles has several advantages [28, 29]. First, rotational alignment is relatively simple to achieve, requiring only acupuncture needles. Second, while we did not demonstrate quantitative tuning here, the degree of alignment might be controlled through the number of rotations or mechanical attachment to the collagen. The alignment relies heavily on adhesion of collagen fibers onto the acupuncture needle. Future work might include optimizing the needle surface in order to tune the mechanical linkage between the needle and the collagen network. This linkage may be dependent on size, material, and geometry of the needle which has yet to be studied with respect to alignment of collagen networks. Third, this approach allows for local manipulation of the collagen fiber alignment. Many of the other techniques mentioned in the introduction result in global alignment of collagen or other ECM. Several of these advantages can be leveraged to understand or control the behavior of cells in ECM. For instance, in the tumor microenvironment (TME), collagen is frequently present in combination with other ECM components such as fibronectin and hyaluronan. Since it is relatively easy to simultaneously image the collagen field during rotation, propagation lengths of collagen alignment in these composite environments with various types and degrees of crosslinking would give a clearer picture of the micromechanical properties of the ECM in the TME. An important note to make is that this method does have limitations as a model. The ECM within the tumor is much more complex and includes a number of cellular and ECM species, which are not currently addressed. Having said this, the contact guidance behavior we see does correlate with invasion and metastasis seen in side-by-side comparisons of the cell lines used here [34]. Since we use a PDMS pad to steady the needle during rotation, it is likely that this approach could be easily combined with microfluidic chambers that present gradients across 3D gels, migration responses to multi-cue environments like those present in the TME could be assessed [21]. Because of the local nature of this alignment approach, different combinations of directional cues (parallel, orthogonal, etc.) could be probed simultaneously.

Along with the potential to use this contact guidance system in other contexts, we show in this paper that MDA-MB-231 cells sense contact guidance cues and MTLn3 cells do not. Several previous papers have indicated that different cell types sense 2D contact guidance cues differently. We and others have attributed this to motility mode, particularly in the context of cancer cell migration [6-8, 35]. Our previous work conducted using epitaxially grown collagen fibrils, a 2D contact guidance cue, resulted in MDA-MB-231 cells, a mesenchymal mode migrator, showing a high directionality while MTLn3 cells, an amoeboid mode migrator, showed low directionality [7]. Directionality measured in the 2D system is about 2 fold higher than that measured in the 3D system here. Two possible explanations seem

reasonable. First, the contact guidance cue is only presented to the ventral plasma membrane, allowing for a more robust cytoskeletal organization along the fiber alignment direction [36]. Second, the degree of fiber alignment in 3D is less than that in 2D. Recently, another group has indicated that motility mode difference explains variation in 3D contact guidance fidelity [8]. Cancer stem cells with more amoeboid like morphology poorly follow contact guidance cues, whereas mesenchymal mode cells follow the directional cue well. What causes this difference between motility modes? It is likely the adhesion characteristics. Mesenchymal cells which adhere to the ECM more firmly can extend protrusions along collagen fibers and stay in physical contact with the ECM for longer times. Amoeboid cells on the other hand follow the pore structure. However, it is not obvious if there is anisotropy of pore orientations or sizes in aligned collagen fiber networks. Cells are known to move in paths where matrix has been degraded [37], but in the absence of mesenchymal cells that actively degrade the matrix and that engage in contact guidance, it is unlikely that these directional pores exist. This diversity in response of mesenchymal and amoeboid cells likely impacts our understanding of metastasis. Because cells don't respond similarly to the same aligned ECM cue, predicting metastasis may depend on knowing the motility mode. Appropriate adhesion, contraction or matrix degradation biomarkers of motility mode could be used. However, it has also been shown that cancer cells are relatively plastic and can switch motility modes [37]. Consequently, ECM alignment may select from one or several motile populations of cancer cells for cells that use the mesenchymal mode of motility [3]. This selection results in a different population of cells as secondary sites and might require different therapeutic approaches.

When plotting cell migration speed vs. directionality, one can see that speed and directionality are not necessarily coupled processes as has been observed in 1D migration [38]. We see similar effects in 2D, where directionality and speed can be jointly or individually controlled depending on the perturbation [6]. The directionality of MTLn3 cells did not increase upon radial fiber alignment (2π). However, the speed did (Figure 9B). Furthermore, glycation (g) produced about the same speed increases as radial fiber alignment. Both the mechanical properties of the aligned fiber field as well as the local density could be higher. Others have reported about a 5-fold increase in Young's modulus in aligned fiber fields [20]. In addition, we noticed slight increases in the signal of collagen close to the needle placement. This agrees with previous reports that indicate that radial alignment by acupuncture needles increases local collagen density [28]. The change in elastic or compressive modulus seen with glycation is on the order of 3-10 fold [32], so speed changes with collagen alignment could be associated with changes in elastic or compressive modulus. It is interesting to note that the changes in speed appear to be additive as glycated (g), aligned collagen fibers (2π) result in the largest speed (Figure 9B). Consequently, MTLn3 cells under our control conditions likely reside on the upslope of the biphasic migration speed curve. MDA-MB-231 cells increase their speed in both glycated and aligned collagen networks, however the response is not

additive (Figure 9C). Perhaps MDA-MB-231 cells are closer to the migration maximum, so increasing the stiffness by both glycating and aligning the collagen network actually results in a lower migration speed due to crossing over the maximum on the biphasic migration speed curve.

While collagen glycation acts to increase speed, it also has interesting effects on directionality. Aligned collagen fibers that are glycated (g) and that are consequently stiffer act to diminish contact guidance fidelity when compared to collagen alone (Figure 9C). Why do stiffer environments result in a directionality decrease? Cells appear to locally organize collagen fibers when migrating through collagen networks [39-41]. This may act as an amplification mechanism turning a modestly aligned collagen network into highly aligned cell migration, resulting in high directionality. If the environment is stiffer, this amplification mechanism may be diminished leading to lower directionality. In addition, matrix degradation can act to soften the local environment [42]. Consequently, inhibiting matrix degradation would act to decrease the ability of cells to locally rearrange collagen fibers resulting in lower directionality. Indeed, we have seen that the addition of TIMPs act to degrade directionality in 3D with perhaps more modest effects on 2D contact guidance cues [43].

Finally, as in 2D environments, it appears that myosin II regulatory light chain phosphorylation through Rho kinase has a substantial role in tuning contact guidance fidelity. When myosin II is partially inhibited with sub-maximal doses of blebbistatin [6], there is a small decrease in both speed and directionality (Figure 9D). However when Rho kinase is partially inhibited with sub-maximal doses of Y-27632 [6], directionality is dramatically altered. This may indicate that Rho kinase is critically important during migration of mesenchymal cells in 3D. Contractility, through Rho kinase has long been known to be important in migration [44-47]. Myosin contractility is not required for the initial stages of spreading [48] and other cytoskeletal proteins that govern protrusion can modulate contact guidance [49]. However, we and others have recently shown Rho-kinase's role in modulating directionality in contact guidance separate from migration speed [6, 20]. Rho kinase inhibition decreases contact guidance fidelity [6, 20], likely by altering adhesion through focal adhesions [35]. This is potentially interesting as contractility is likely modulated by soluble factors in the TME, creating the possibility that contact guidance response can be attenuated. Thus, contact guidance depends intimately on the degree of alignment of the ECM, however different cells respond differently to contact guidance cues and both extracellular factors like ECM stiffness as well as intracellular factors like Rho kinase-mediated contractility can modulate the contact guidance response.

5. Conclusions:

We have investigated contact guidance in 3D using an effective method of radially aligning collagen fibers towards a rotated acupuncture needle. MDA-MB-231 (mesenchymal) cells show a high degree of directional response to the contact guidance cue while MTLn3 (amoeboid) cells do not migrate directionally, behavior that is seen in 2D contact guidance systems. However, MTLn3 cells were not immune to changes in migration. Cell speed increased when the collagen network was aligned or when the stiffness was increased through glycation, suggesting additional changes in the collagen network occur separate from collagen fiber alignment after acupuncture needle rotation. In fact, changes in migration speed brought on by collagen alignment seemed to be additive with respect to changes brought on by glycation. Increasing the stiffness of the aligned collagen network by through glycation marginally decreases directionality in MDA-MB-231 cells. However, lowering intracellular contractility, particularly through Rho kinase drastically decreases directionality in MDA-MB-231 cells, but unlike in 2D contact guidance environments cell directionality and speed are more tightly coupled. This suggests modulation of the contractile apparatus more potently affects contact guidance than modulation of extracellular mechanical properties of the contact guidance cue.

Acknowledgements:

We acknowledge Margaret Carter at the Confocal and Multiphoton Facility at Iowa State University with help in imaging samples with confocal reflectance microscopy. Anai Perez was supported by an NSF-REU [1560012]. This work was supported by the National Institutes of Health/National Cancer Institute [R03CA184575] and National Institutes of Health/National Institute for General Medical Sciences [R01GM115672]. The content is solely the responsibility of the authors and does not necessarily represent the official views of the NIH.

References:

[1] Mehlen P, Puisieux A. Metastasis: a question of life or death. Nature Reviews Cancer 2006;6:449-58.
[2] Pankova K, Rosel D, Novotny M, Brabek J. The molecular mechanisms of transition between mesenchymal and amoeboid invasiveness in tumor cells. Cellular and Molecular Life Sciences 2010;67:63-71.
[3] Hecht I, Bar-El Y, Balmer F, Natan S, Tsarfaty I, Schweitzer F, et al. Tumor Invasion Optimization by Mesenchymal-Amoeboid Heterogeneity. Scientific Reports 2015;5.
[4] Provenzano PP, Eliceiri KW, Campbell JM, Inman DR, White JG, Keely PJ. Collagen reorganization at the tumor-stromal interface facilitates local invasion. BMC Med 2006;4.
[5] Balcioglu HE, van de Water B, Danen EHJ. Tumor-induced remote ECM network orientation steers angiogenesis. Scientific Reports 2016;6:12.
[6] Wang J, Schneider IC. Myosin phosphorylation on stress fibers predicts contact guidance behavior across diverse breast cancer cells. Biomaterials 2017;120:81-93.
[7] Wang J, Petefish JW, Hillier AC, Schneider IC. Epitaxially Grown Collagen Fibrils Reveal Diversity in Contact Guidance Behavior among Cancer Cells. Langmuir 2015;31:307-14.
[8] Ray A, Slama ZM, Morford RK, Madden SA, Provenzano PP. Enhanced Directional Migration of Cancer Stem Cells in 3D Aligned Collagen Matrices. Biophysical Journal 2017;112:1023-36.
[9] Nelson CM, Bissell MJ. Of extracellular matrix, scaffolds, and signaling: Tissue architecture regulates development, homeostasis, and cancer. Annual Review of Cell and Developmental Biology 2006;22:287-309.
[10] Ng MR, Brugge JS. A Stiff Blow from the Stroma: Collagen Crosslinking Drives Tumor Progression. Cancer Cell 2009;16:455-7.
[11] Lange JR, Fabry B. Cell and tissue mechanics in cell migration. Experimental Cell Research 2013;319:2418-23.
[12] Hadjipanayi E, Mudera V, Brown RA. Guiding Cell Migration in 3D: A Collagen Matrix with Graded Directional Stiffness. Cell Motility and the Cytoskeleton 2009;66:121-8.
[13] Ni Y, Chiang MYM. Cell morphology and migration linked to substrate rigidity. Soft Matter 2007;3:1285-92.
[14] Doyle AD, Carvajal N, Jin A, Matsumoto K, Yamada KM. Local 3D matrix microenvironment regulates cell migration through spatiotemporal dynamics of contractility-dependent adhesions. Nature Communications 2015;6.
[15] Mason BN, Starchenko A, Williams RM, Bonassar LJ, Reinhart-King CA. Tuning three-dimensional collagen matrix stiffness independently of collagen concentration modulates endothelial cell behavior. Acta Biomaterialia 2013;9:4635-44.
[16] Geiger B, Bershadsky A, Pankov R, Yamada KM. Transmembrane extracellular matrix-cytoskeleton crosstalk. Nature Reviews Molecular Cell Biology 2001;2.
[17] Humphrey JD, Dufresne ER, Schwartz MA. Mechanotransduction and extracellular matrix homeostasis. Nature Reviews Molecular Cell Biology 2014;15:802-12.
[18] Friedl P, Gilmour D. Collective cell migration in morphogenesis, regeneration and cancer. Nature Reviews Molecular Cell Biology 2009;10:445-57.
[19] Lammermann T, Sixt M. Mechanical modes of 'amoeboid' cell migration. Current Opinion in Cell Biology 2009;21:636-44.
[20] Riching KM, Cox BL, Salick MR, Pehlke C, Riching AS, Ponik SM, et al. 3D Collagen Alignment Limits Protrusions to Enhance Breast Cancer Cell Persistence. Biophysical Journal 2014;107:2546-58.
[21] Rodriguez LL, Schneider IC. Directed cell migration in multi-cue environments. Integrative Biology 2013;5:1306-23.
[22] Kolind K, Leong KW, Besenbacher F, Foss M. Guidance of stem cell fate on 2D patterned surfaces. Biomaterials 2012;33:6626-33.

[23] Nisbet DR, Forsythe JS, Shen W, Finkelstein DI, Horne MK. Review Paper: A Review of the Cellular Response on Electrospun Nanofibers for Tissue Engineering. Journal of Biomaterials Applications 2009;24:7-29.
[24] Antman-Passig M, Levy S, Gartenberg C, Schori H, Shefi O. Mechanically Oriented 3D Collagen Hydrogel for Directing Neurite Growth. Tissue Eng Part A 2017;23:403-14.
[25] Dickinson RB, Guido S, Tranquillo RT. Biased Cell Migration of Fibroblasts Exhibiting Contact Guidance in Oriented Collagen Gels. Ann Biomed Eng 1994;22:342-56.
[26] Guo C, Kaufman LJ. Flow and magnetic field induced collagen alignment. Biomaterials 2007;28:1105-14.
[27] Provenzano PP, Inman DR, Eliceiri KW, Trier SM, Keely PJ. Contact Guidance Mediated Three-Dimensional Cell Migration is Regulated by Rho/ROCK-Dependent Matrix Reorganization. Biophysical Journal 2008;95:5374-84.
[28] Julias M, Buettner HM, Shreiber DI. Varying Assay Geometry to Emulate Connective Tissue Planes in an In Vitro Model of Acupuncture Needling. Anat Rec 2011;294:243-52.
[29] Julias M, Edgar LT, Buettner HM, Shreiber DI. An in vitro assay of collagen fiber alignment by acupuncture needle rotation. Biomed Eng Online 2008;7.
[30] Langevin HM, Churchill DL, Cipolla MJ. Mechanical signaling through connective tissue: a mechanism for the therapeutic effect of acupuncture. Faseb J 2001;15:2275-82.
[31] Puspoki Z, Storath M, Sage D, Unser M. Transforms and Operators for Directional Bioimage Analysis: A Survey. In: DeVos WH, Munck S, Timmermans JP, editors. Focus on Bio-Image Informatics. Berlin: Springer-Verlag Berlin; 2016. p. 69-93.
[32] Roy R, Boskey A, Bonassar LJ. Processing of type I collagen gels using nonenzymatic glycation. Journal of Biomedical Materials Research2010. p. 843-51.
[33] Bailey AJ, Sims TJ, Avery NC, Halligan EP. Non-enzymic glycation of fibrous collagen: reaction products of glucose and
ribose. Biochem J. Great Britain1995. p. 385-90.
[34] Zhou ZN, Sharma VP, Beaty BT, Roh-Johnson M, Peterson EA, Van Rooijen N, et al. Autocrine HBEGF expression promotes breast cancer intravasation, metastasis and macrophage-independent invasion in vivo. Oncogene 2014;33:3784-93.
[35] Ray A, Lee O, Win Z, Edwards RM, Alford PW, Kim DH, et al. Anisotropic forces from spatially constrained focal adhesions mediate contact guidance directed cell migration. Nature Communications 2017;8.
[36] Case LB, Waterman CM. Integration of actin dynamics and cell adhesion by a three-dimensional, mechanosensitive molecular clutch. Nature Cell Biology 2015;17:955-63.
[37] Friedl P, Wolf K. Tumour-cell invasion and migration: Diversity and escape mechanisms. Nature Reviews Cancer 2003;3:362-74.
[38] Maiuri P, Terriac E, Paul-Gilloteaux P, Vignaud T, McNally K, Onuffer J, et al. The first World Cell Race. Curr Biol 2012;22:R673-R5.
[39] Barocas VH, Tranquillo RT. An anisotropic biphasic theory of tissue-equivalent mechanics: The interplay among cell traction, fibrillar network deformation, fibril alignment, and cell contact guidance. J Biomech Eng-Trans ASME 1997;119:137-45.
[40] Wu PH, Giri A, Sun SX, Wirtz D. Three-dimensional cell migration does not follow a random walk. Proc Natl Acad Sci U S A 2014;111:3949-54.
[41] Hall MS, Alisafaei F, Ban E, Feng XZ, Hui CY, Shenoy VB, et al. Fibrous nonlinear elasticity enables positive mechanical feedback between cells and ECMs. Proc Natl Acad Sci U S A 2016;113:14043-8.
[42] Xu C, Wang C, Cai QF, Zhang Q, Weng L, Liu GM, et al. Matrix Metalloproteinase 2 (MMP-2) Plays a Critical Role in the Softening of Common Carp Muscle during Chilled Storage by Degradation of Type I and V Collagens. Journal of Agricultural and Food Chemistry 2015;63:10948-56.

[43] Lee KB, Nam DH, Nuhn JAM, Wang J, Schneider IC, Ge X. Direct expression of active human tissue inhibitors of metalloproteinases by periplasmic secretion in Escherichia coli. Microbial Cell Factories 2017;16.
[44] Brabek J, Mierke CT, Rosel D, Vesely P, Fabry B. The role of the tissue microenvironment in the regulation of cancer cell motility and invasion. Cell Communication and Signaling 2010;8.
[45] Sahai E, Marshall CJ. RHO-GTPases and cancer. Nature Reviews Cancer 2002;2:133-+.
[46] Friedl P. Prespecification and plasticity: shifting mechanisms of cell migration. Current Opinion in Cell Biology 2004;16:14-23.
[47] Wolf K, Friedl P. Molecular mechanisms of cancer cell invasion and plasticity. British Journal of Dermatology 2006;154:11-5.
[48] Sales A, Holle AW, Kemkemer R. Initial contact guidance during cell spreading is contractility-independent. Soft Matter 2017;13:5158-67.
[49] Ramirez-San Juan GR, Oakes PW, Gardel ML. Contact guidance requires spatial control of leading-edge protrusion. Mol Biol Cell 2017;28:1043-53.

Figure Legends:

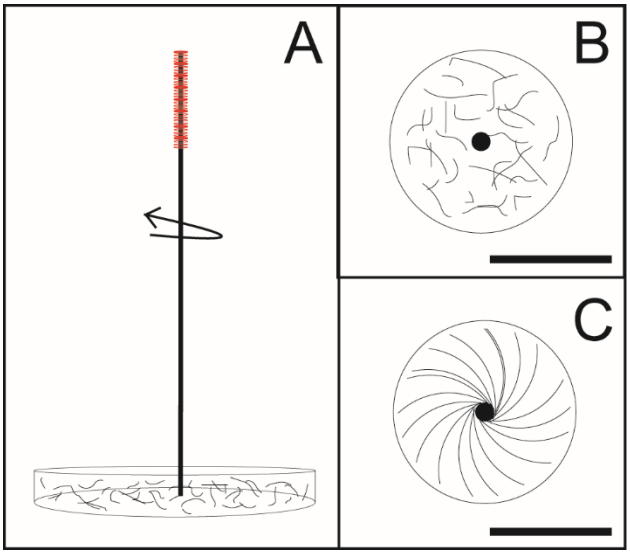

Figure 1: Schematic of aligned collagen gels. (A) An acupuncture needle is inserted into a collagen gel and rotated. A top view of the needle in the gel (B) before rotation and (C) after rotation. The scale bars are 1 cm.

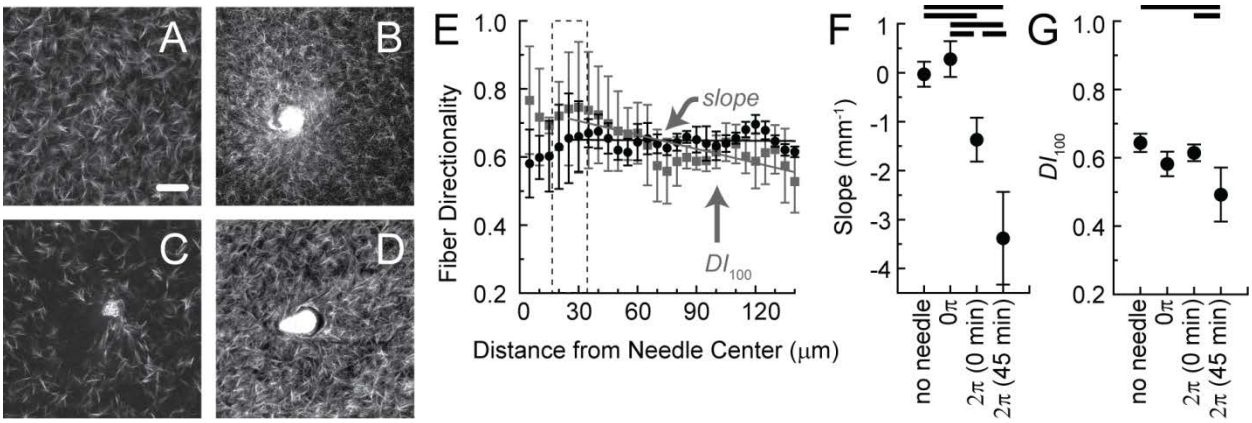

Figure 2: Confocal reflectance microscopy images of the alignment of the collagen gel under different needle conditions. Image of a fully polymerized collagen gel with (A) no needle, (B) a needle which has been inserted but not rotated (0π), (C) a needle which has been rotated (2π) prior to complete collagen polymerization (0 min) and (D) a needle which has been rotated (2π) at 45 min after the start of collagen polymerization. The scale bar is 50 μm. (E) Fiber directionality as a function of distance from the needle center for a gel with no needle (black circles) and a needle that has been rotated prior to complete collagen polymerization (grey squares). A linear fit of the fiber directionality from 25-140 μm is shown as a solid line, yielding a slope used in (F). An average fiber directionality centered 100 μm from the center of the needle (DI_{100}) is marked with an arrow and used in (G). The dotted line represents the average needle radius +/- one standard deviation. The (F) slope of the fiber directionality curve for each conditions and (G) average fiber directionality centered 100 μm from the center of the needle (DI_{100}) for the conditions shown in (A-D). The error bars represent 95% confidence intervals of the mean ($N_{gels} > 4$). Significance bars represent non-overlapping confidence intervals.

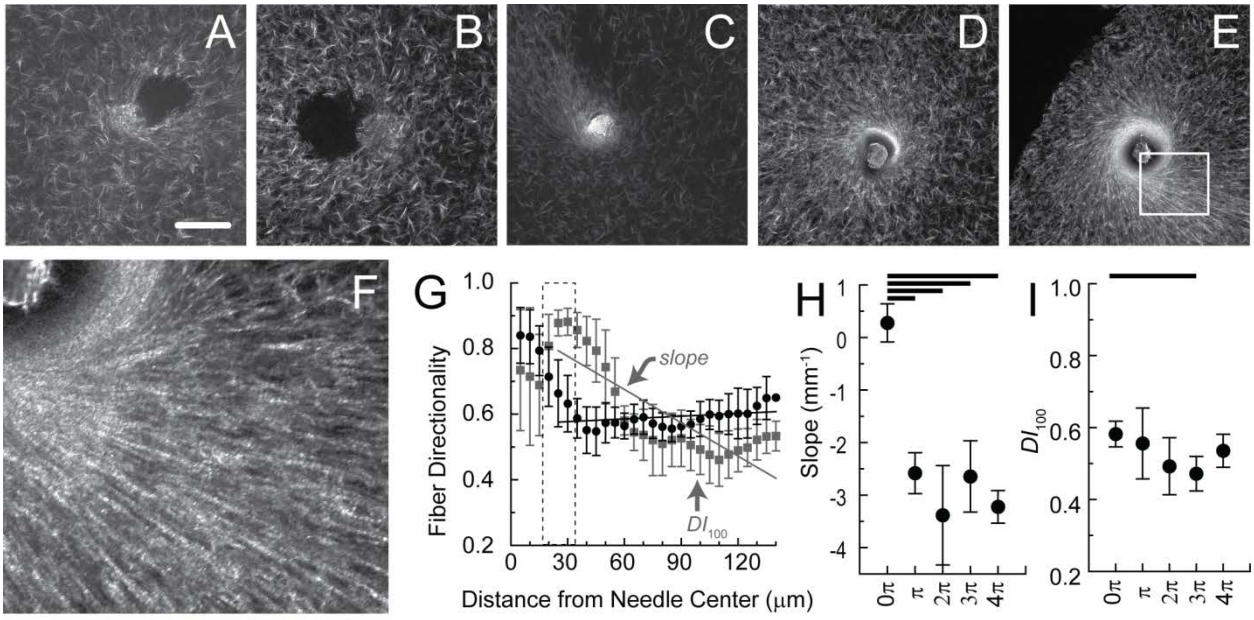

Figure 3: Confocal reflectance microscopy images of the alignment of the collagen gel under different numbers of rotations. Image of a fully polymerized collagen gel rotated (A) 0π, (B) π, (C) 2π, (D) 3π, and (E) 4π. The scale bar is 50 μm. A zoomed region in (E) is shown in (F). (G) Fiber directionality as a function of distance from the needle center for a gel rotated 0π (black circles) and 2π (grey squares). A linear fit of the fiber directionality from 25-140 μm is shown as a solid line, yielding a slope used in (H). An average fiber directionality centered 100 μm from the center of the needle (DI_{100}) is marked with an arrow and used in (I). The dotted line represents the average needle radius +/- one standard deviation. The (H) slope of the fiber directionality curve for each conditions and (I) average fiber directionality centered 100 μm from the center of the needle (DI_{100}) for the conditions shown in (A-E). The error bars represent 95% confidence intervals of the mean (N_{gels} = 5). Significance bars represent non-overlapping confidence intervals.

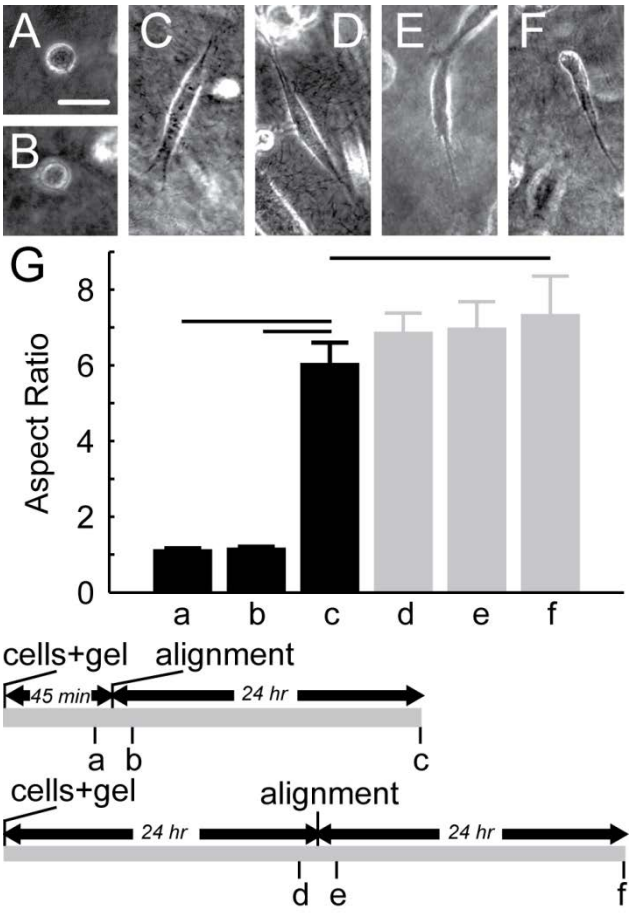

Figure 4: Aspect ratios of MDA-MB-231 cancer cells. Phase contrast images of MDA-MB-231 cells (A) before 2π, (B) after 2π, (C) at ~24 hr after 2π needle rotation at $t = 0$, (D) before 2π, (E) after 2π, and (F) at ~24 hr after 2π needle rotation at $t = 24$ hr. The scale bar is 50 μm. (G) Aspect ratios of conditions shown in (A-F). The experimental scheme is shown below. The error bars represent 95% confidence intervals of the mean ($N_{experiments} = 3$, $N_{cells} > 300$). Lines represent statistical significance using an Anova test, $p \leq 0.05$.

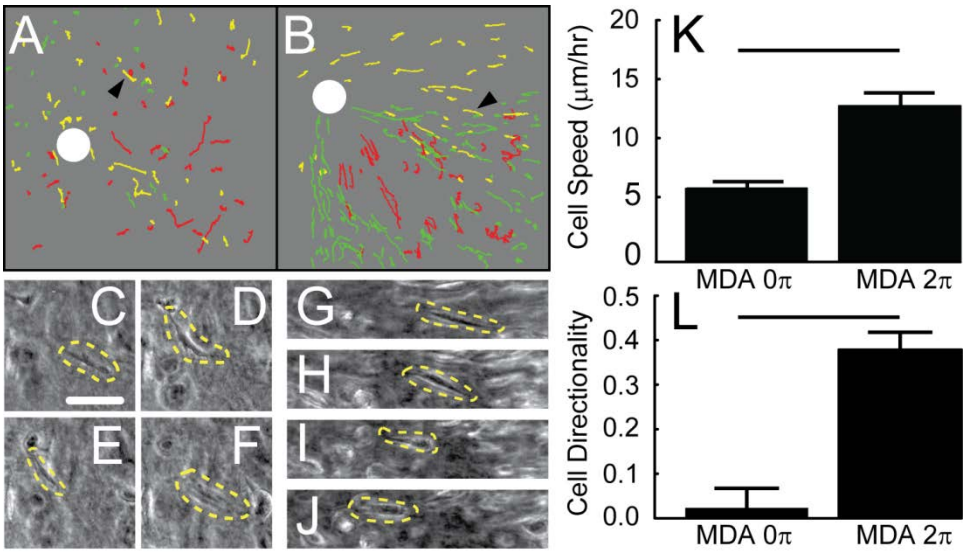

Figure 5: Cell migration analysis of MDA-MB-231 cells. MDA-MB-231 cell tracks for (A) 0π and (B) 2π needle rotations. White circles indicate needle locations, while different colors (green, red and yellow) represent different experiments. The diameter of the circle is about 60 μm. Phase contrast images of MDA-MB-231 cells migrating in a collagen gel rotated by (C-F) 0π or (G-J) 2π taken at time 0, 2, 4, and 6 hr and outlined with a yellow dashed line. The scale bar is 50 μm. (K) Cell speed and (L) directionality of the cells in collagen gels rotated 0π and 2π. Error bars are 95% confidence intervals of the mean ($N_{experiments}$ = 3 and N_{cells} > 105). Lines represent statistical significance using a two tailed *t*-test, $p \leq 0.05$.

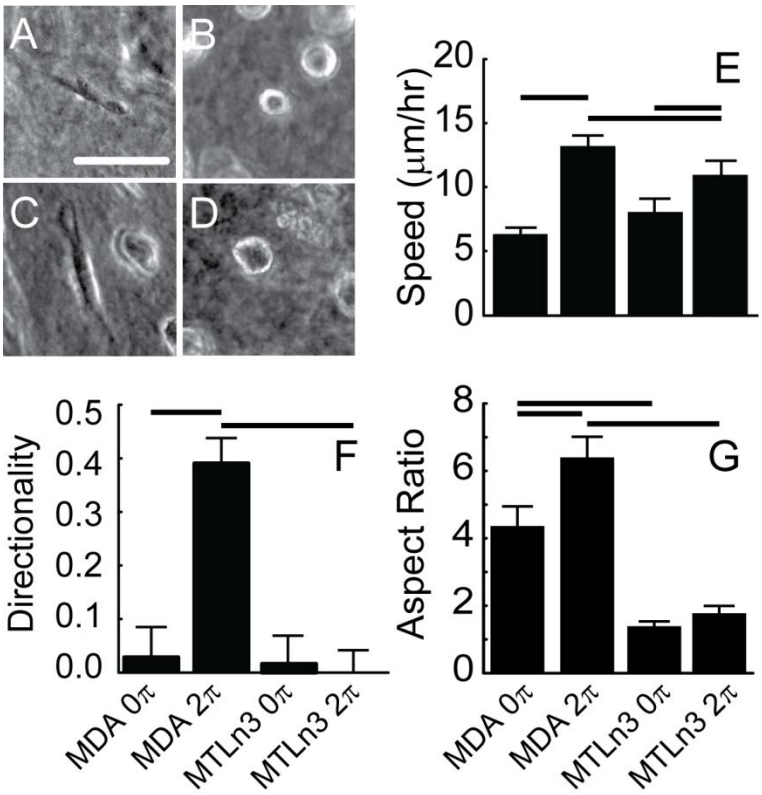

Figure 6: Comparing contact guidance of MDA-MB-231 and MTLn3 cells. Phase contrast images of (A&C) MDA-MB-231 and (B&D) MTLn3 cells in a collagen gel rotated by (A&B) 0π or (C&D) 2π. The scale bar is 50 μm. Cell (E) speed, (F) directionality, and (G) aspect ratio. Error bars are 95% confidence intervals of the mean ($N_{experiments}$ = 3 and N_{cells} > 105). Lines represent statistical significance between conditions with at least one common condition parameter using an Anova test, $p \leq 0.05$.

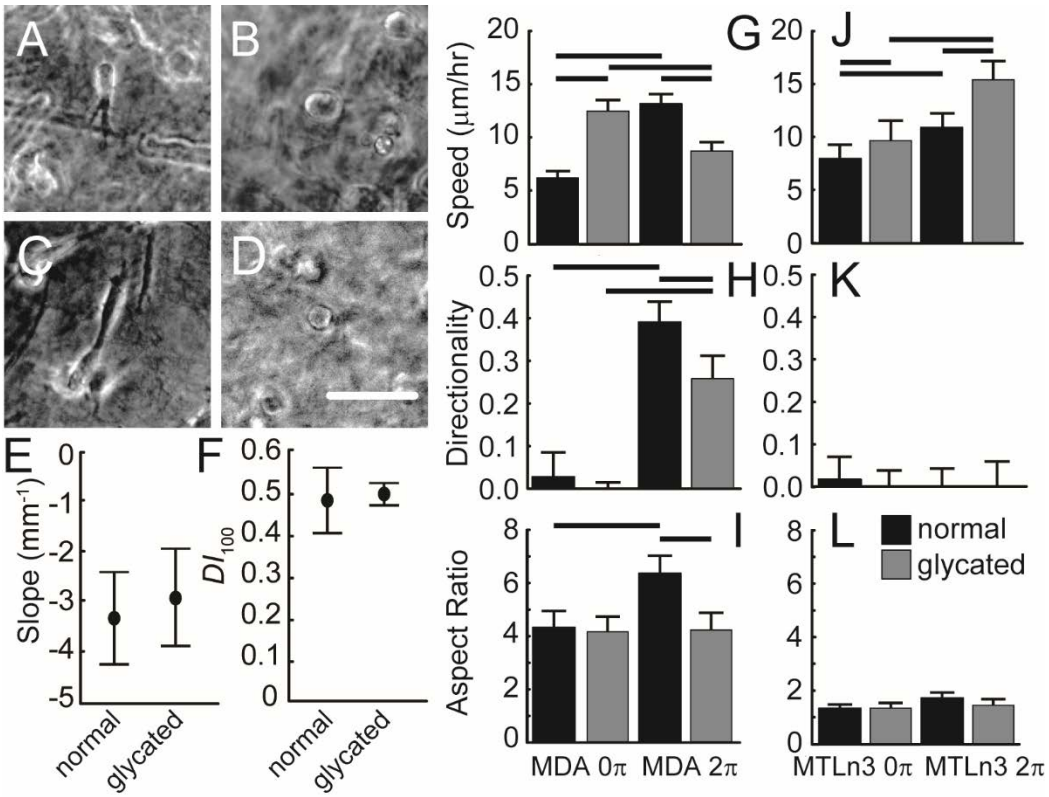

Figure 7: Comparing MDA-MB-231 cells and MTLn3 cells in glycated collagen matrices. Phase contrast images of (A&C) MDA-MB-231 and (B&D) MTLn3 cells in a glycated collagen gel rotated by (A&B) 0π or (C&D) 2π. The scale bar is 50 μm. Normal and glycated collagen (E) slope and (F) directionality 100 μm away from the center of the needle (DI_{100}) are calculated as done previously (N_{gels}= 4). Cell (G&J) speed, (H&K) directionality, and (I&L) aspect ratio. Error bars are 95% confidence intervals of the mean ($N_{experiments}$ = 3 and N_{cells} > 105). Lines represent statistical significance between conditions with at least one common condition parameter using an Anova test, $p \leq 0.05$.

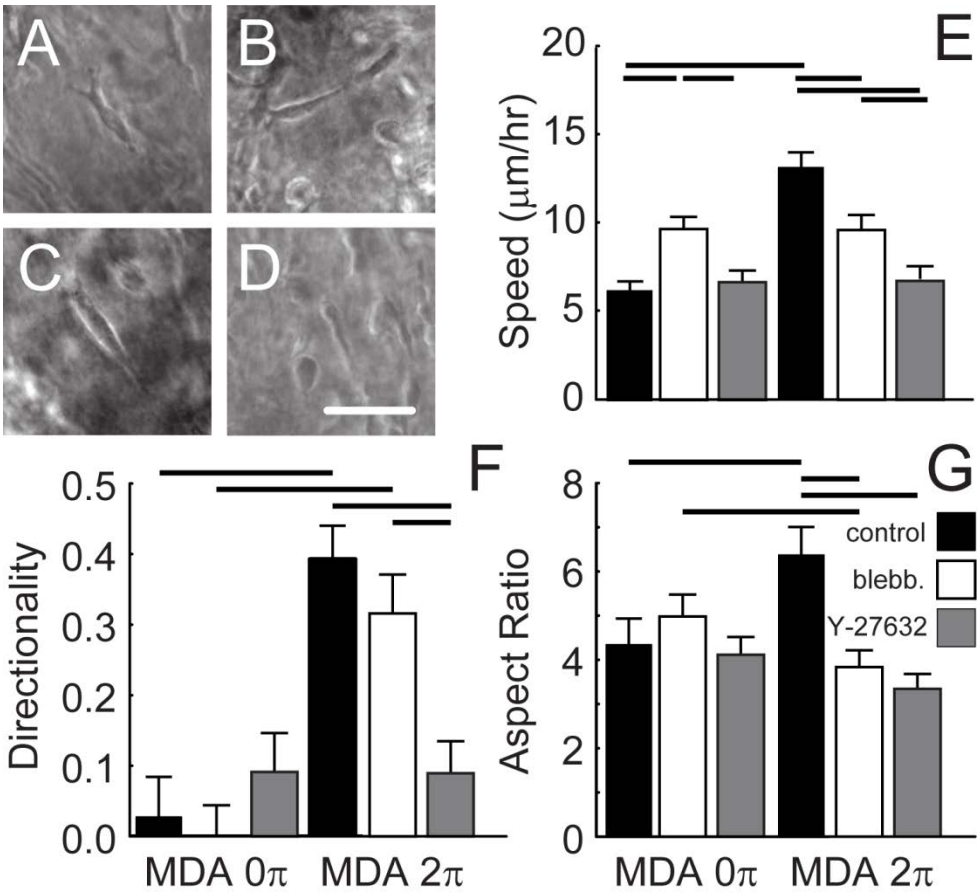

Figure 8: Examining the effect of contractility inhibitors on MDA-MB-231 cells. Phase contrast images of MDA-MB-231 cells in unaligned (A&B) and aligned (C&D) collagen networks treated with 3 μM Blebbistatin (A&C) or 1 μM Y-27632 (B&D). The scale bar is 50 μm. Cell (E) speed, (F) directionality, and (G) aspect ratio. Error bars are 95% confidence intervals of the mean ($N_{experiments}$ = 3 and N_{cells} > 105). Lines represent statistical significance between conditions with at least one common condition parameter using an Anova test, $p \leq 0.05$.

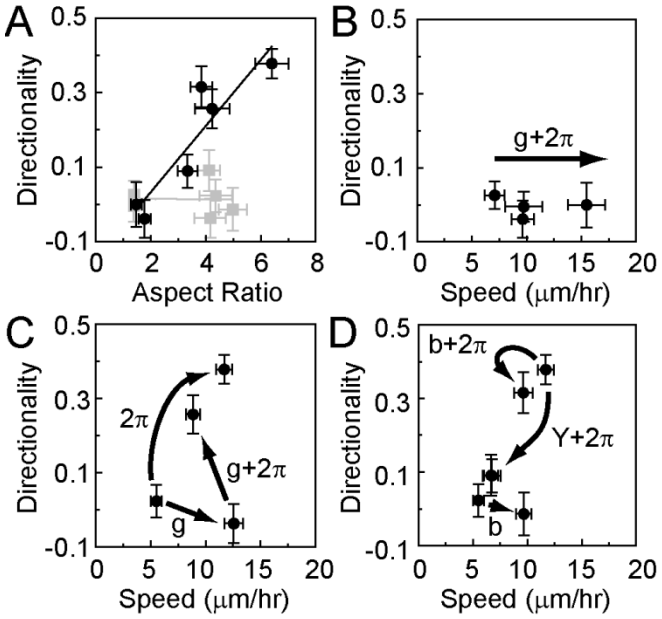

Figure 9: Compilation of speed, directionality and aspect ratio across all conditions. These data are replicated from previous figures and presented differently. (A) Directionality and aspect ratio for aligned (black) and unaligned (grey) across control, glycated collagen and contractility inhibited MDA-MB-231 and MTLn3 cells. (B) Directionality and speed for MTLn3 cells under glycation (g) and aligned (2π) conditions. (C) Directionality and speed for MDA-MB-231 cells under glycation (g) and aligned (2π) conditions. (D) Directionality and speed for MDA-MB-231 cells under blebbistatin (b), Y-27632 (Y) and aligned (2π) conditions. Error bars are 95% confidence intervals of the mean ($N_{experiments}$ = 3 and N_{cells} > 105).